Supplementary information

The disordered region 1 of Mdm2 weakens p53-binding in both its hyperphospho- and unmodified-forms

Yingyue Luo,[1] Jehanne Procaccia,[1,2] Chafiaa Bouguechtouli,[1] Ania Alik,[1] Magali Aumont-Nicaise,[1] Francois-Xavier Theillet*[,1,2]
[1] Université Paris-Saclay, CEA, CNRS, Institute for Integrative Biology of the Cell (I2BC), 91198 Gif-sur-Yvette, France.
[2] Université Paris Cité, CNRS, CiTCoM, F-75006 Paris, France.
* E-mail: francois-xavier.theillet@cnrs.fr

Mdm2-IDR1 conservation among vertebrates

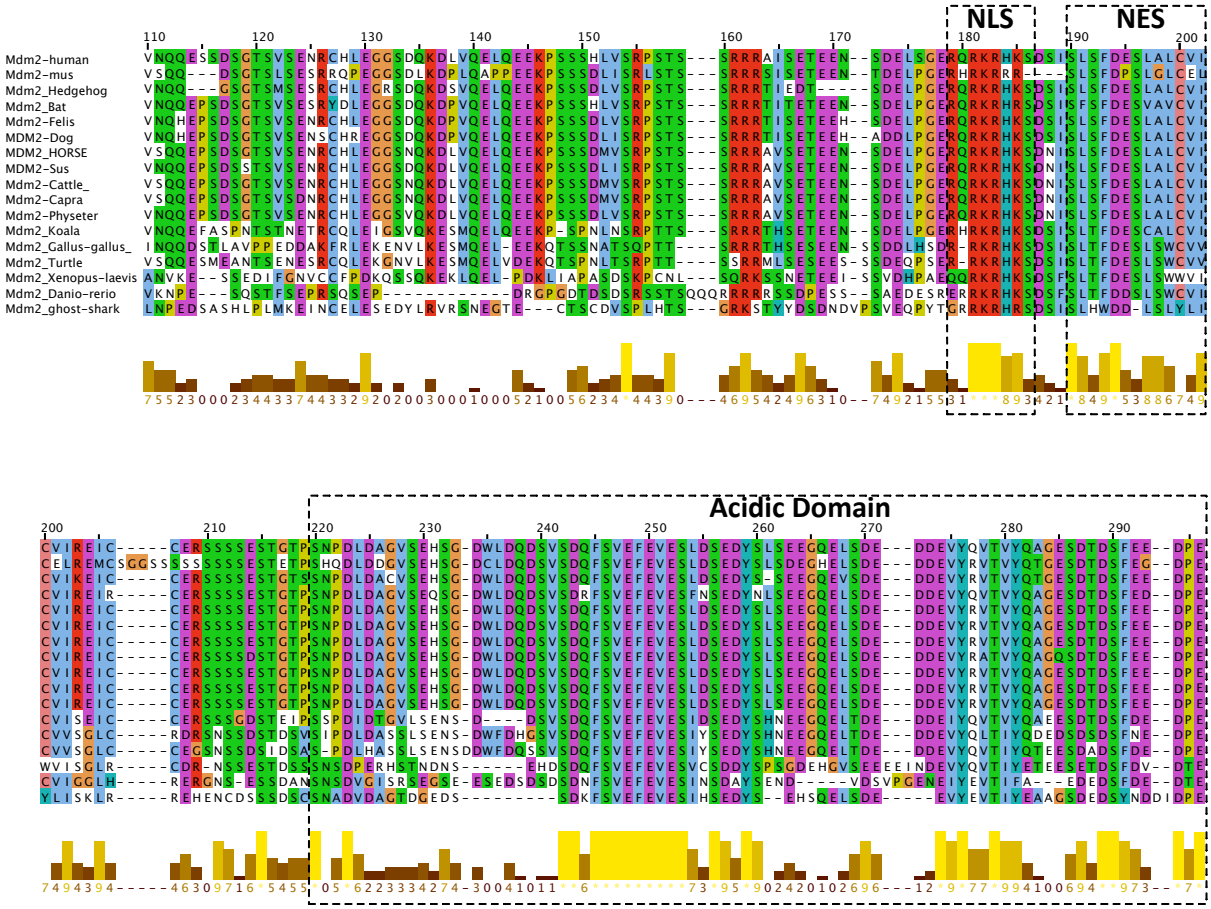

Supplementary Figure 1: *Protein sequence alignment of Mdm2-IDR1 among representative vertebrates, created using JalView* [1] *and aligned using MAFFT* [2,3].

```
Mdm2-human      MCNTNMSVPTDGAVTTSQIPASEQETLVRPKPLLLKLLKSVGAQKDTYTMKEVLFYLGQY     60
MdmX            MTSFSTSAQCSTSDS-ACRISPGQINQVRPKLPLLKILHAAGAQGEMFTVKEVMHYLGQY     59
                * . . *.  . : : :   :  * . ****  ***:*::.*** : :*:***:.*****

Mdm2-human      IMTKRLYDEKQQHIVYCSNDLLGDLFGVPSFSVKEHRKIYTMIYRNLVVVNQQESSDSGT     120
MdmX            IMVKQLYDQQEQHMVYCGGDLLGELLGRQSFSVKDPSPLYDMLRKNLVTLATATTDAAQT     119
                **.*:***:::**:***..****:*:*  *****:   :* *: :***.:    :. : *

Mdm2-human      SVSENRCHLEGGSDQKDLVQELQEEKPS-----SSHLVSRPSTSSRRRAISETEENSDEL     175
MdmX            LALA-QDHSMDIPSQDQLKQSAEESSTSRKRTTEDDIPTLPTS--EHKCIHS-REDEDLI     175
                 .   : *  .  .*.:* *. :*.. *     ...: : *::  .::.* . .*:.* :

Mdm2-human      SGERQRKRHKSDSISLSFDES----LALCVI---REICCERSSSSESTGTPSNPDLDAG-     227
MdmX            ENLA---QDETSRLDLGFEEWDVAGLPWWFLGNLRSNYTPRSNG--STDLQTNQDVGTAI     230
                ..     :.::. :.*.*:*     *   .:   *.    **..  **.  :* *:.:.

Mdm2-human      -VSEHSGDWLDQDSVSDQFSVEFEVESLDSEDYSLSEEGQELSDEDDEVYQVTVYQAGE-     285
MdmX            VSDTTDDLWFLNESVSEQLGVGIKVEAADTEQTSEE--V-------GKVSDKKVIEVGKN     281
                  .  .. *: ::***:*:.* ::**: *:*: * .          .:* : .* :.*:

Mdm2-human      -----SDTDSFEEDPEISLADYWKCTSCNEMNPPLPSHCNRCWALRENWLPEDKGKDKGE     340
MdmX            DDLEDSKSLSDDTDVEVTSEDEWQCTECKKFNSPSKRYCFRCWALRKDWYSDCSKLTHS-     340
                     *.: * : * *::  * *:**.*:::* *   :* ******::*  : .   :.

Mdm2-human      ISEKAKLENSTQAEEGFDVPDCKKTIVNDSR---ESCVEENDDKITQASQSQESEDYSQP     397
MdmX            LSTSDITAIPEKENEGNDVPDCRRTISAPVVRPKDAYIKKENSKLFDPCNSVEFLDLAHS     400
                :* .       : :** *****::**        :: ::::::.*: : .:* *  * ::

Mdm2-human      STSSSIIYSSQEDVKEFEREETQDKEESVESSLPLNAIEPCVICQGRPKNGCIVHGKTGH     457
MdmX            SESQETISSMGEQLDNLSEQR----TDTENMEDCQNLLKPCSLCEKRPRDGNIIHGRTGH     456
                * *.. * *  *::.::.:.:.     :: : .   * ::** :*: **::* *:**:***

Mdm2-human      LMACFTCAKKLKKRNKPCPVCRQPIQMIVLTYFP  491
MdmX            LVTCFHCARRLKKAGASCPICKKEIQLVIKVFIA  490
                *::** **::*** .  **:*:: **::: .::
```

Supplementary Figure 2: *Protein sequence alignment of human Mdm2 and MdmX, using Clustal Omega [4]; the WW and WF motifs of MdmX binding to MdmX-p53BD domain are highlighted in yellow and green, respectively -as determined in previous studies by Daughdrill, Chen and colleagues [5], and Rainey and colleagues [6]; the corresponding Mdm2 fragments binding to Mdm2-p53BD are colored in the same colors; hydrophobic residues in these segments are shown in bold; the folded domains of Mdm2 are highlighted in grey.*

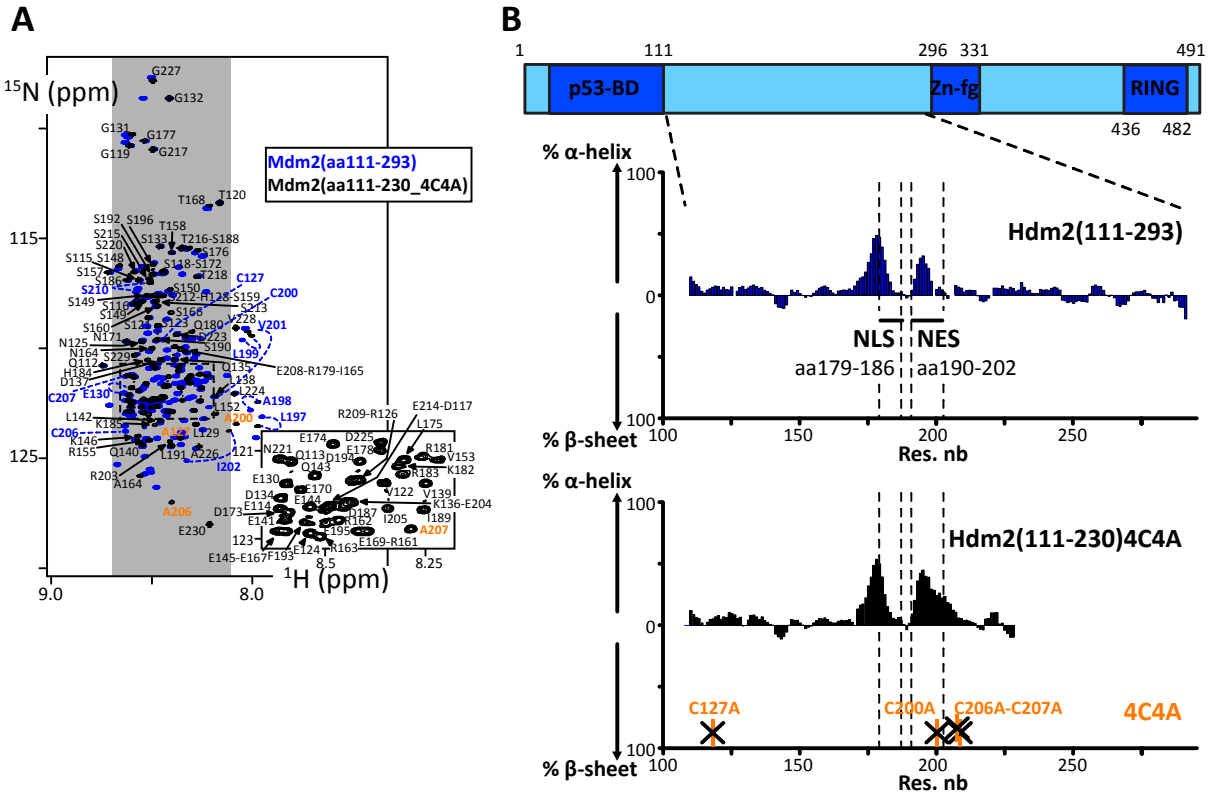

Supplementary Figure 3: A. *Overlay of 2D ^{1}H–^{15}N HSQC spectra (700 MHz, 283 K, pH 7.0) of Mdm2(aa111-293) in black, Mdm2(aa111-230_4C4A) in blue; only the assignment of Mdm2(aa111-230_4C4A) is shown, with Cys-to-Ala noticeable changes in blue and the new Ala in orange; the inset is a close-up view of the crowded area (dotted square) in the middle of the spectra;* ***B.*** *Primary structure of Mdm2, and secondary structure propensities of Mdm2(aa1-293) and Mdm2(aa111-230_4C4A), calculated from the assigned Cα-Cβ and using ncSPC [7,8]; the positions of point mutations are indicated in orange.*

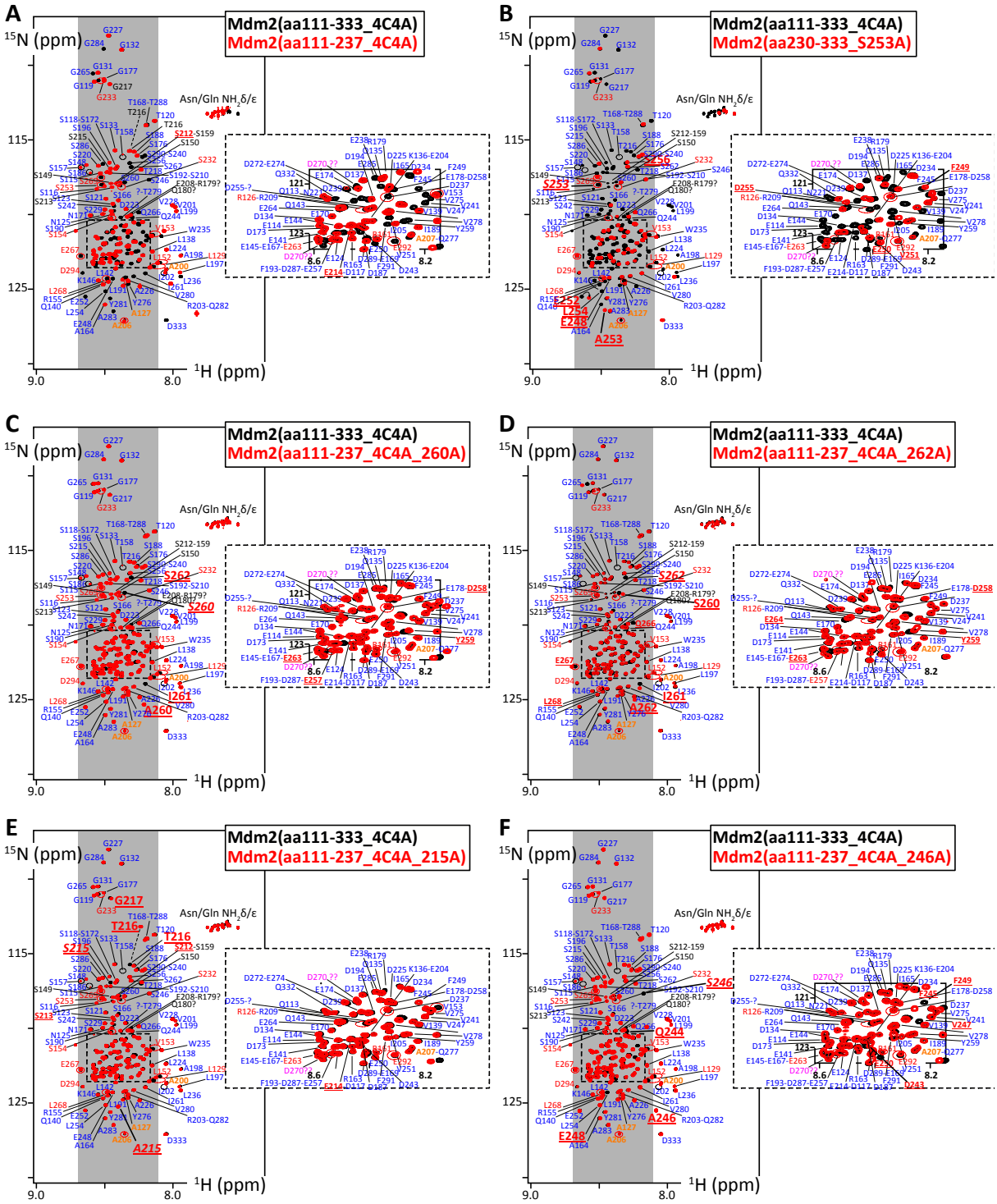

Supplementary Figure 4: A-F. *Overlays of 2D ^{1}H–^{15}N HSQC spectra (700 MHz, 283 K, pH 7.0) of Mdm2(aa111-333_4C4A) and of a list of truncated and/or mutated constructs; the remarkable changes in the spectra are labelled in red; the grey zone represents the window where random coil residues resonate usually; the insets are close-up views of crowded area (dotted squares) in the middle of the spectra.*

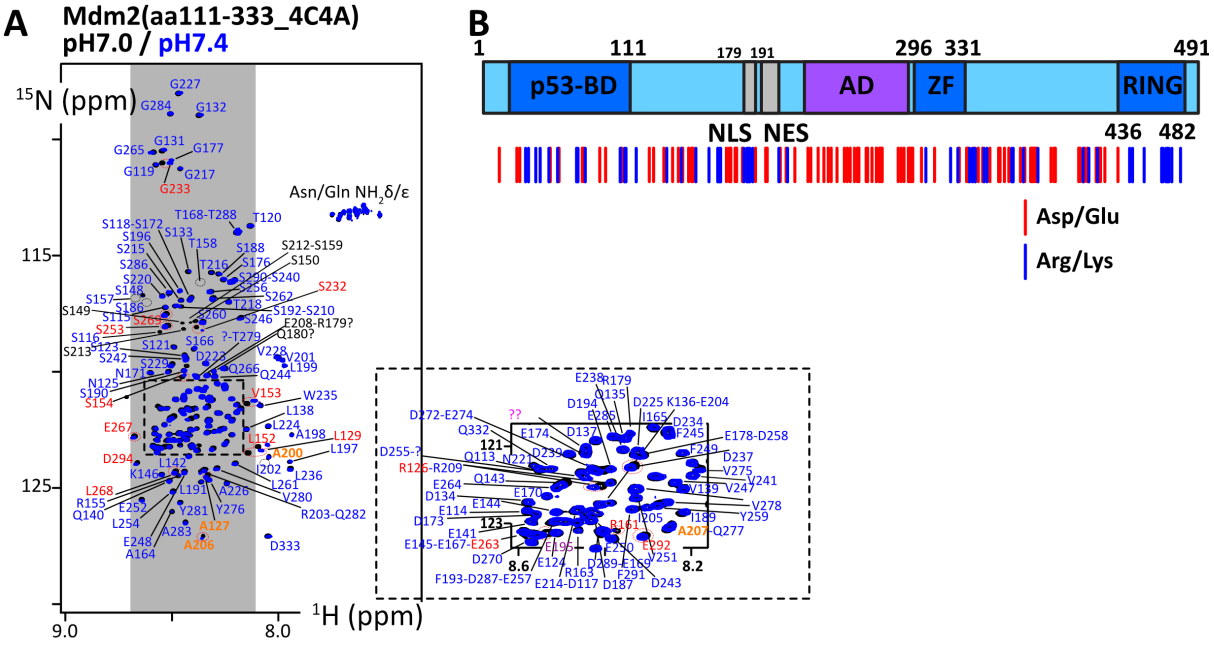

Histidines: H128, H151, H184, H231, H318

Supplementary Figure 5: A. *Overlay of 2D ^{1}H–^{15}N HSQC spectra (700 MHz, 283 K) of Mdm2(aa111-333_4C4A) at pH 7.0 (black) and pH 7.4 (blue); the inset is a close-up view of the crowded area (dotted square) in the middle of the spectra;* ***B.*** *Primary structure of Mdm2, with the positions of negatively (red) and positively (blue) charged amino acids.*

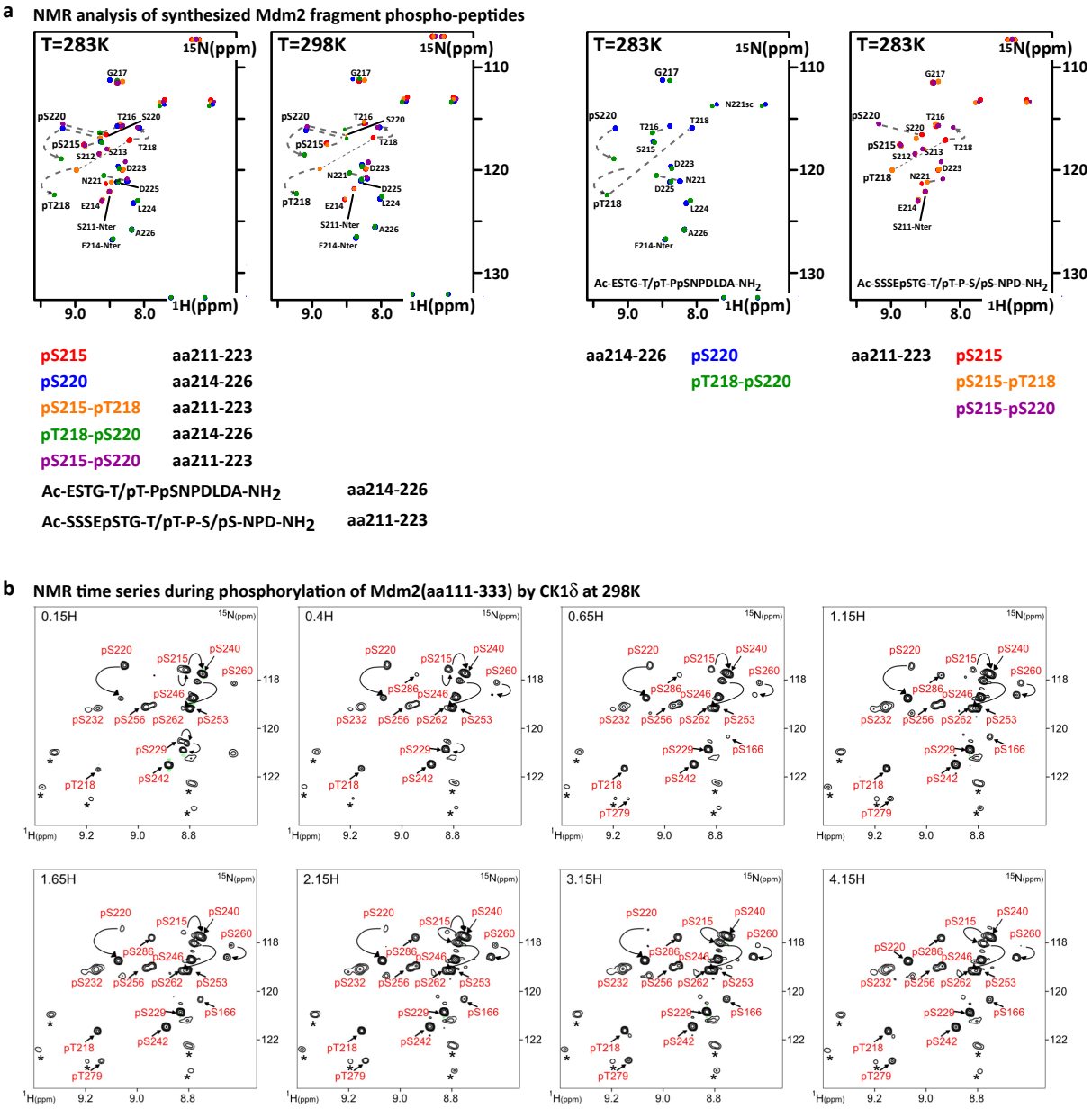

Supplementary Figure 6: a. *Overlays of 2D ^{1}H–^{15}N HSQC spectra (600 MHz, 283 or 298 K) of synthesized peptides corresponding to fragments of Mdm2, aa214-226 and aa211-223, carrying various combinations of phosphorylation on S215, T218 and S220; it shows that pS215 chemical shifts are poorly dependent on T218 and S220 phosphorylation (and vice versa), while pT218 and pS220 crosspeaks do shift substantially in function of the phosphorylation status of each other; this permitted us to conclude that T218 phosphorylation is much slower than S215 and S220, and that pT218-only does almost not exist;* ***b.*** *Close-up views of NMR 2D ^{1}H–^{15}N HSQC spectra (phosphopeaks area) at different times during the phosphorylation of Mdm2(aa111-333) by CK1δ; stars indicate peaks from the Zinc-finger; these spectra show the much faster appearance of pS220(T218) in comparison to pS220(pT218), or the concomitant emergence of both pS260(S262) and pS260(pS262) ending with a near complete pS260(pS262) population; altogether, all these phosphorylation events develop in parallel, in a distributive fashion.*

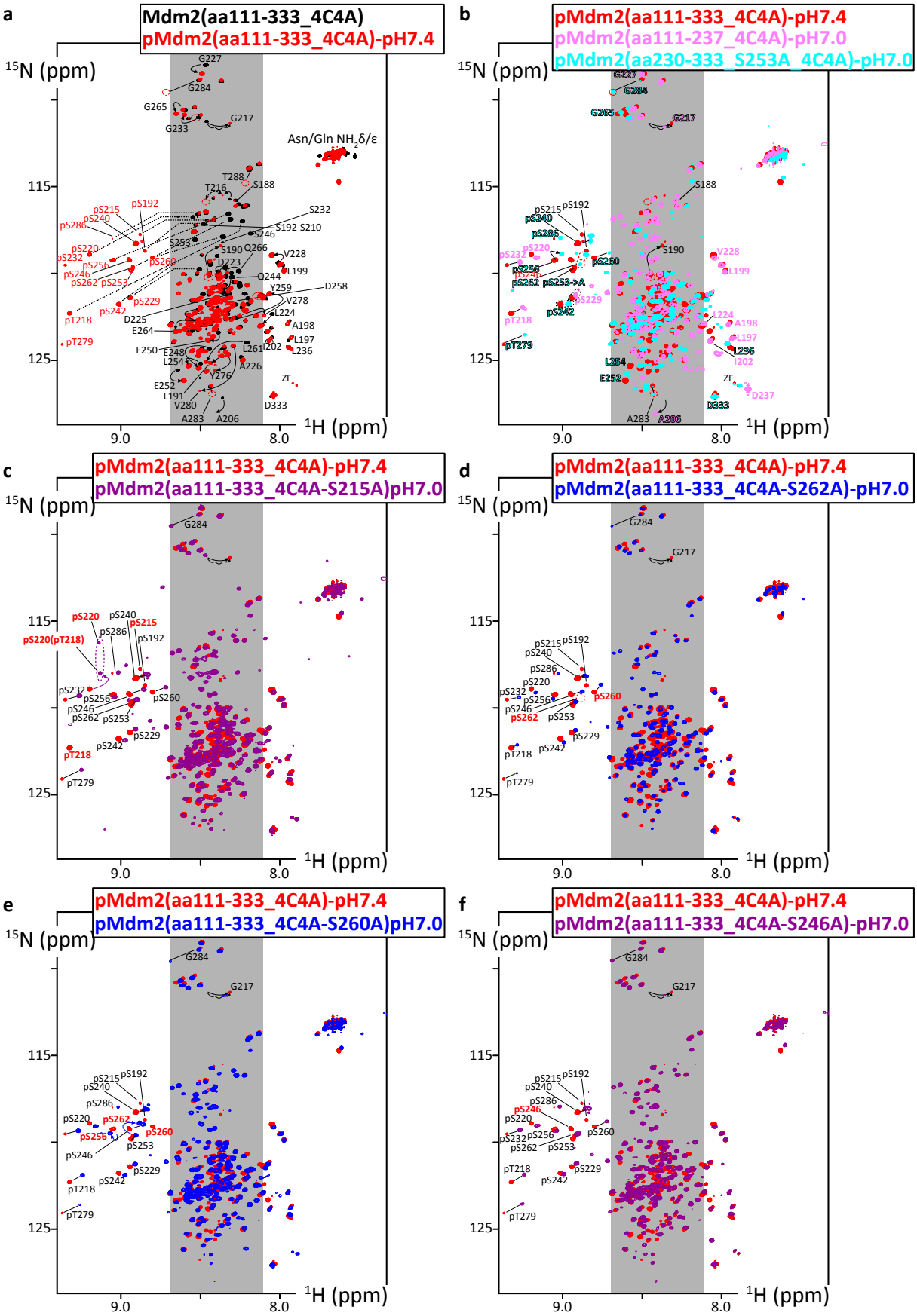

Supplementary Figure 7: *Overlays of 2D ^{1}H–^{15}N HSQC spectra (700 MHz, 283 K) of CK1δ-phosphorylated Mdm2(aa111-333) or mutants thereof; red-bold labels indicate the peaks or the absence of peaks helping the assignment of the WT construct; the WT was at pH 7.4, while*

the mutants are at pH7.0 (lower pH provides more intense NMR peaks), which explains the chemical shifts perturbations of the phosphopeaks due to their partial re-protonation; pS215 generates always a low-intensity signal and is often too weak to be visible in the spectra of the mutants at this contour level; pS192 is not visible in the spectra of the mutants because the phosphorylation reactions have been stopped before its population is large enough.

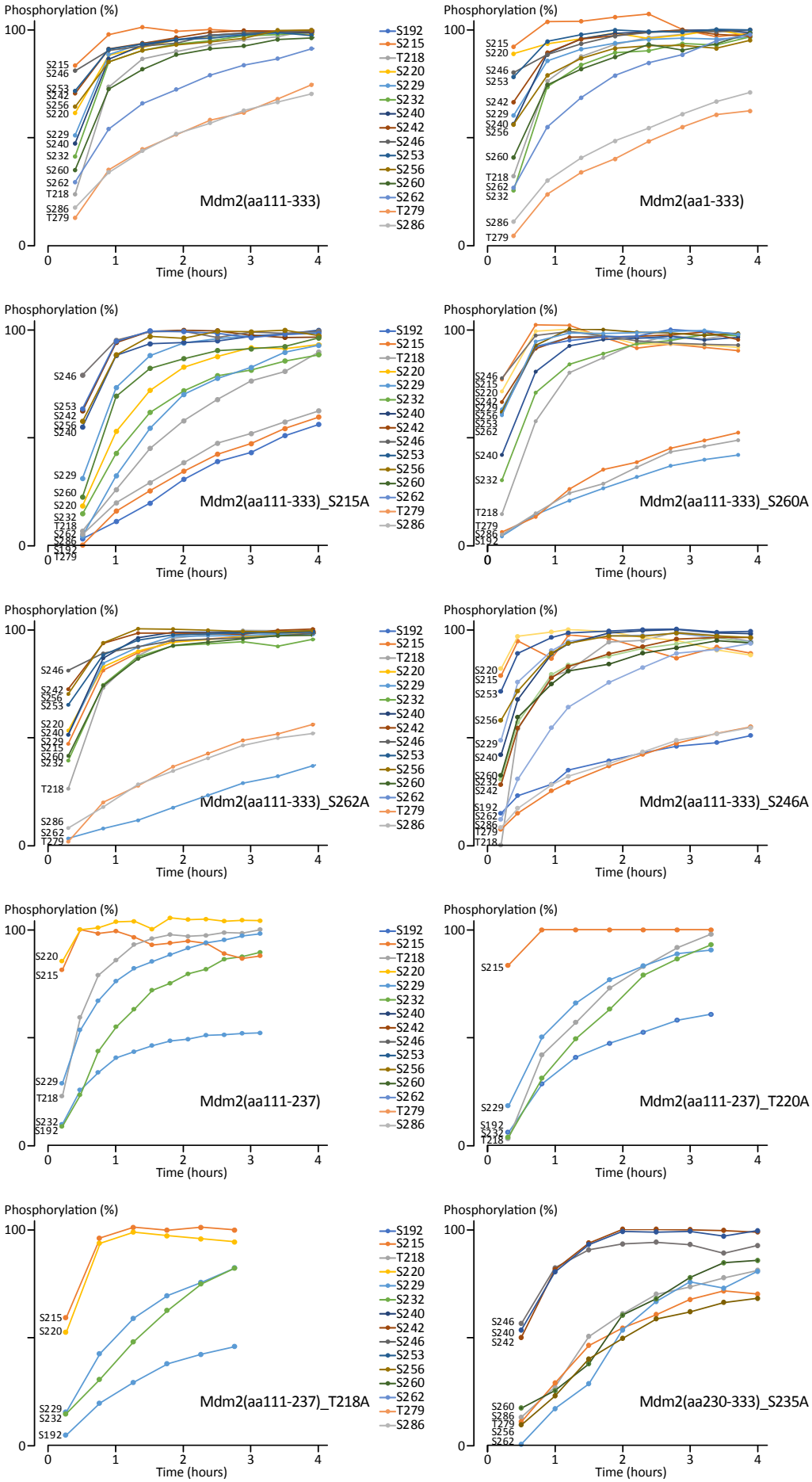
Phosphorylation (%)
100
0
Time (hours)
0
1
2
3
4
Mdm2(aa111-333)
Mdm2(aa1-333)
Mdm2(aa111-333)_S215A
Mdm2(aa111-333)_S260A
Mdm2(aa111-333)_S262A
Mdm2(aa111-333)_S246A
Mdm2(aa111-237)
Mdm2(aa111-237)_T220A
Mdm2(aa111-237)_T218A
Mdm2(aa230-333)_S235A
S192
S215
T218
S220
S229
S232
S240
S242
S246
S253
S256
S260
S262
T279
S286

Supplementary Figure 8: *Phosphorylation kinetics of various constructs of Mdm2 showing residue-specific build-up curves; the experiments have been carried out using CK1δ at 2 μM, Mdm2 peptides at 100 μM, at pH 7.0 and 298 K; the color code is homogeneous through all the graphs.*

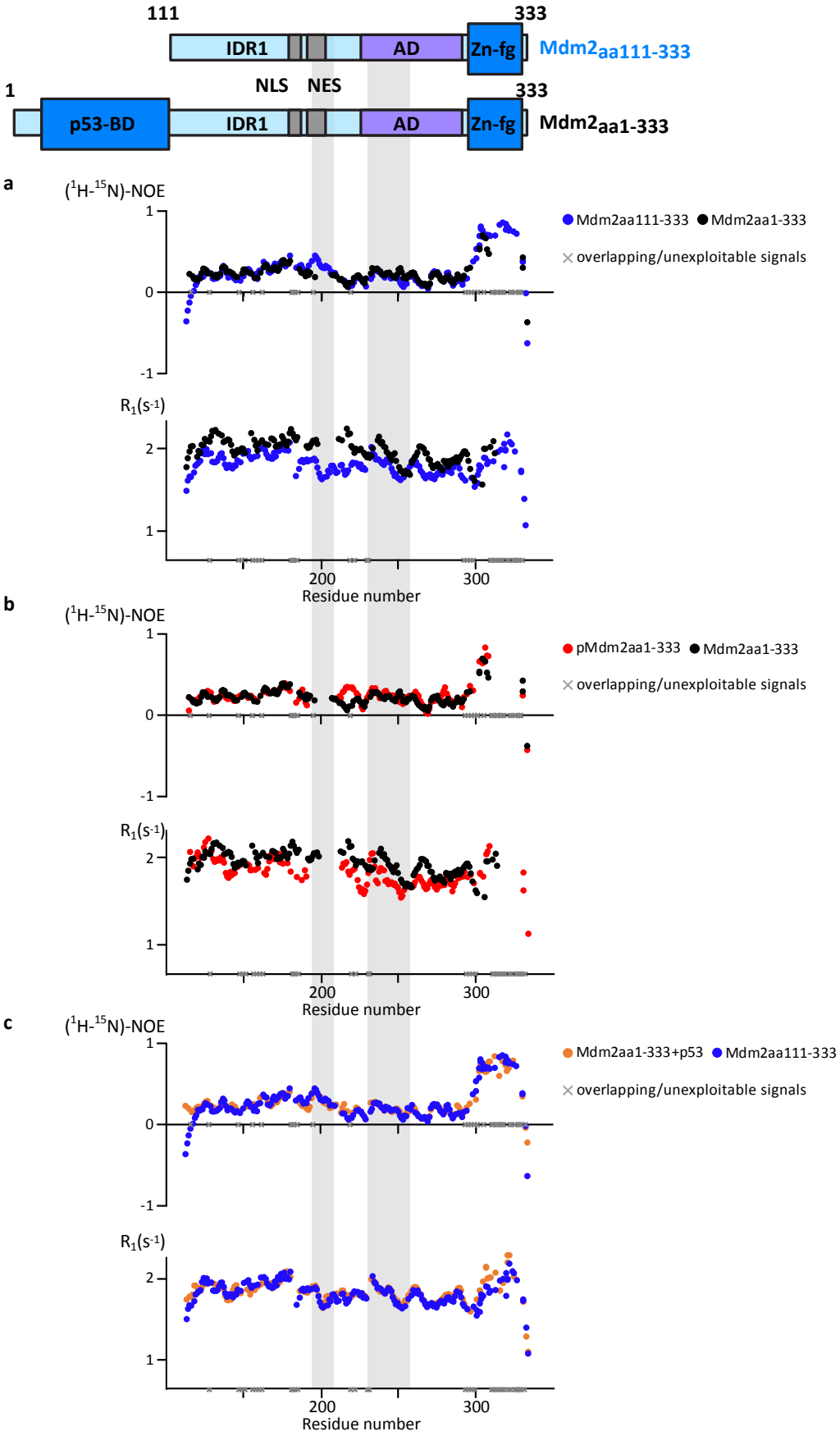

Supplementary Figure 9: *Residue-specific ^{1}H-^{15}N heteronuclear NOEs and ^{15}N-R_1 relaxation rates (700 MHz, 283K, pH 7.4) along the IDR1 and Zinc-finger for* ***a.*** *Mdm2(aa111-333) and Mdm2(aa1-333) (blue and black, respectively),* ***b.*** *Mdm2(aa1-333) and phospho-Mdm2(aa1-*

333) (black and red, respectively), ***c.*** *Mdm2(aa1-333)+p53(aa14-29) and Mdm2(aa111-333) (orange and blue, respectively). The* ^{15}N-R_2 *rates are shown in Figure 2. The error bars from two independent samples are approximately the size of the dots in the graphs.*

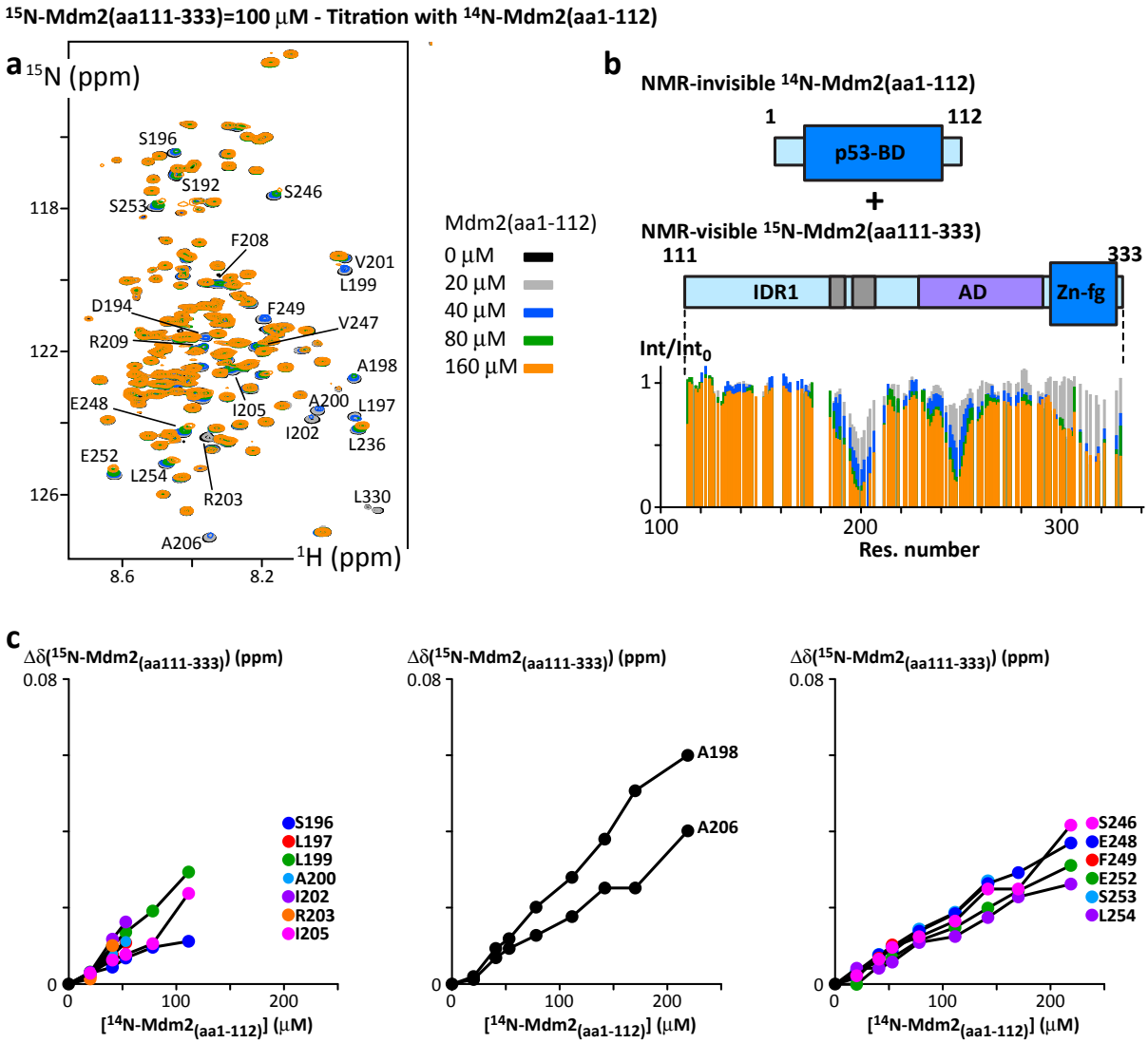

Supplementary Figure 10: a. *Overlay of ^{1}H-^{15}N HSQC spectra (283 K, PBS pH7.0, 600 MHz) of ^{15}N-Mdm2(aa111-333) at 100 µM initially, in presence of growing concentrations of ^{14}N-Mdm2(aa1-112);* ***b.*** *Residue specific ratios of peak intensities from ^{1}H-^{15}N HSQC spectra of ^{15}N-Mdm2(aa111-333) in presence ^{14}N-Mdm2(aa1-112);* ***c.*** *Chemical shift perturbations (CSPs) of ^{15}N-Mdm2(aa111-333) residues in function of the concentration of ^{14}N-Mdm2(aa1-112); the graph on the left shows CSPs of peaks that cannot be tracked through the whole titration because they merge with neighboring peaks or they vanish.*

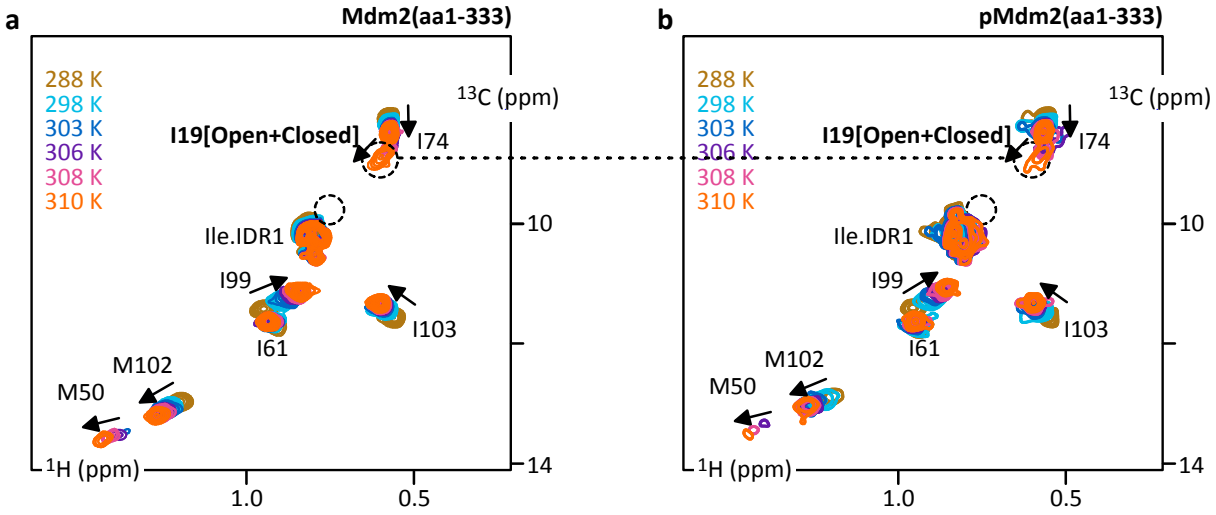

Supplementary Figure 11: a. *Overlay of ^{1}H-^{13}C SOFAST-HMQC methyl-TROSY spectra of Mdm2(aa1-333) at varying temperatures;* ***b.*** *Overlay of ^{1}H-^{13}C SOFAST-HMQC methyl-TROSY spectra of phosphoMdm2(aa111-333) after CK1δ-mediated phosphorylation at varying temperatures; phosphoMdm2(aa111-333) was repurified and separated from CK1d, following the protocol descried in the Material and Methods ; both samples are [u-^{2}D,Ileδ1-Metε-$^{13}CH_3$]-labeled and spectra were recorded at 700 MHz; Mdm2(aa1-333) spectra were recorded at 70 μM, while pMdm2(aa1-333) were recorded at 15 μM, explaining the lower quality of the latter ones.*

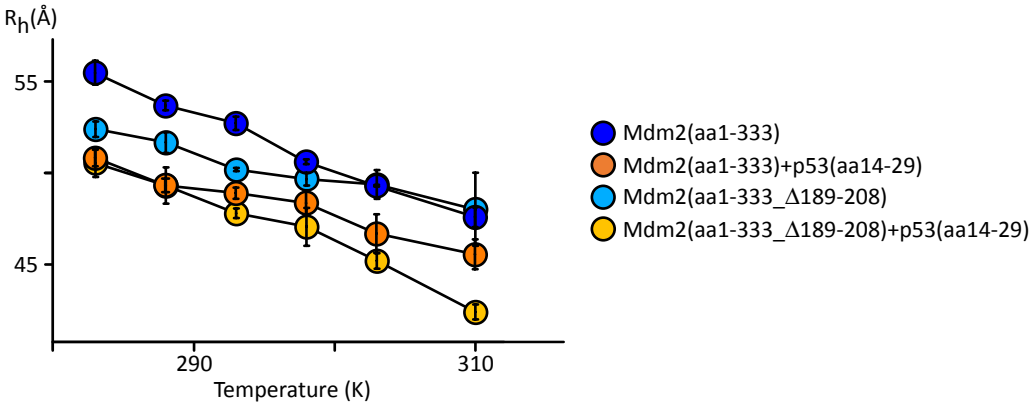

Supplementary Figure 12: *Hydrodynamic radii (R_h) of Mdm2(aa1-333) (blue), of the complex Mdm2(aa1-333)+p53(aa14-29) (orange), of Mdm2(aa1-333_Δ189-208), and of the complex Mdm2(aa1-333_Δ189-208)+p53(aa14-29) (yellow) as a function of temperature, as extracted from the NMR measurements of diffusion rates.*

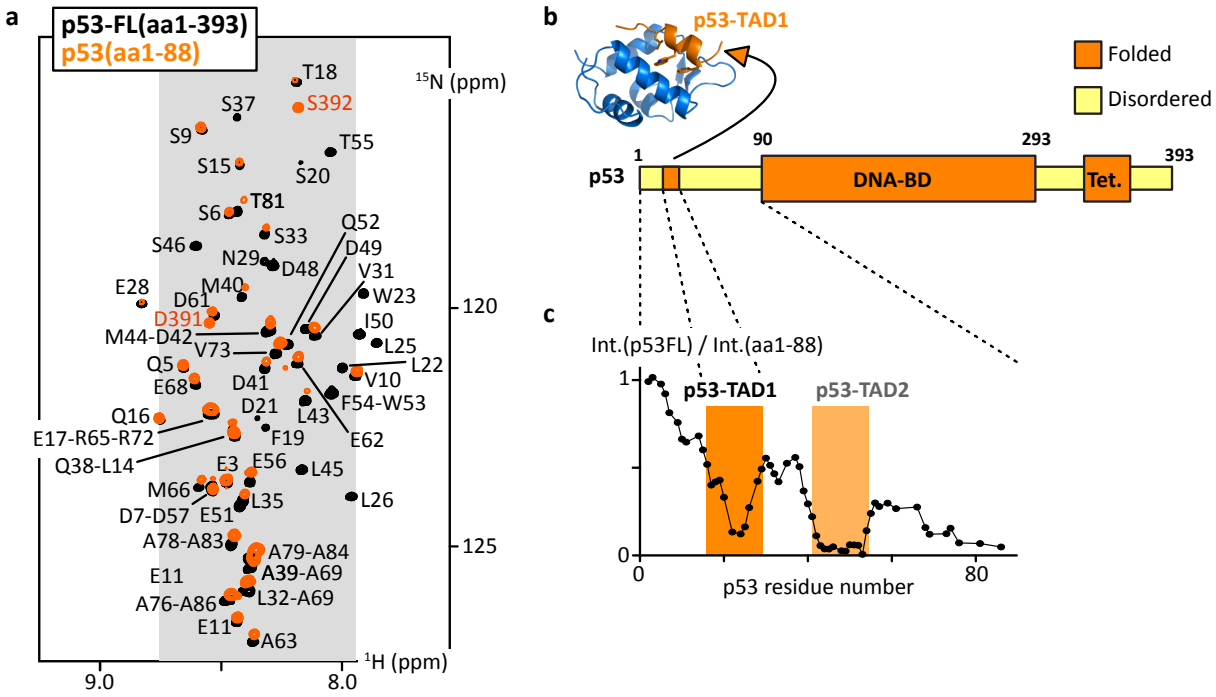

Supplementary Figure 13: a. *Overlay of 2D ^{1}H–^{15}N HSQC spectra (600 MHz, 283 K) of p53-FL(aa1-393) and p53(aa1-88) in black and orange, respectively;* ***b.*** *Primary structure of p53, showing the disordered and folded (or "folding-upon-binding" for p53(aa17-29)) domains in yellow and orange, respectively (DNA-BD: DNA-binding domain; Tet.: tetramerization domain);* ***c.*** *Residue-specific intensity ratios between p53FL and p53(aa1-88) in 2D ^{1}H–^{15}N HSQC spectra; the fragment p53(aa17-29) is also called Transactivation domain 1 (TAD1); the two regions TAD1 and TAD2 show pronounced intensity losses in p53FL, which correspond to intramolecular interactions with the DNA-BD; these compete with DNA-binding and with Mdm2-binding.*

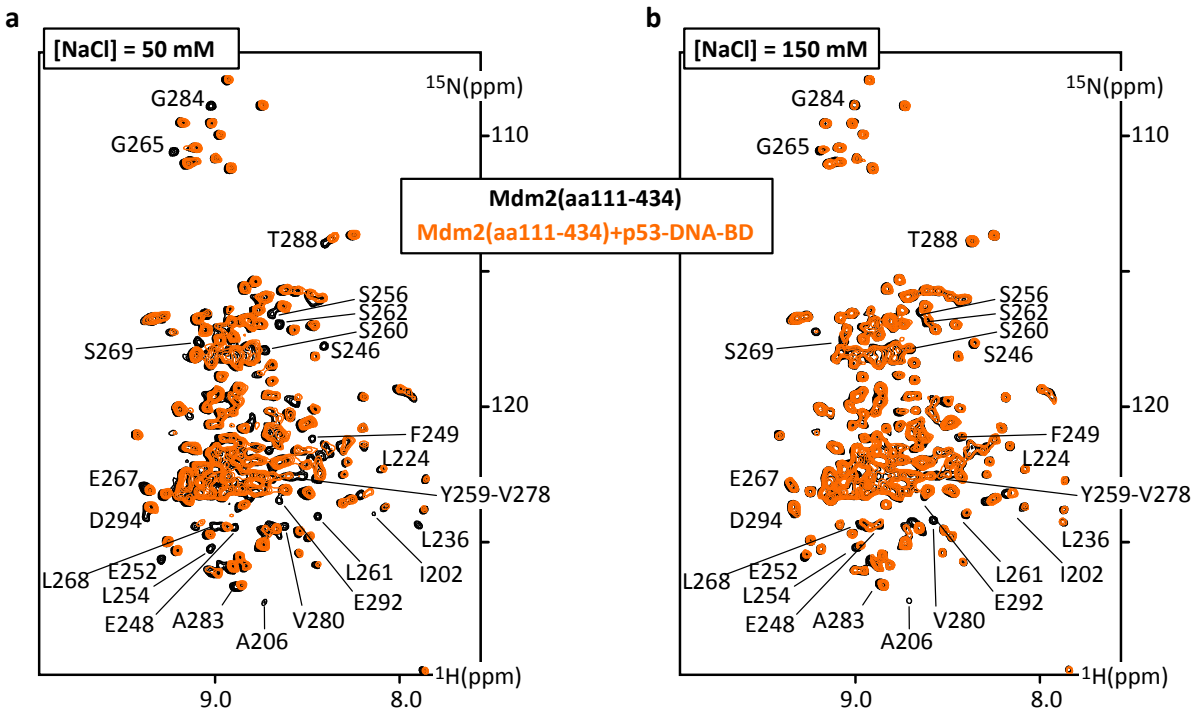

Supplementary Figure 14: *Overlay of 2D ^{1}H–^{15}N HSQC spectra (700 MHz, 283 K) of Mdm2(aa111-434) and of Mdm2(aa111-434)+p53-DNA-BD(aa90-293) (equimolar at 20 μM) in black and orange respectively in a buffer containing either* ***a.*** *NaCl at 50 mM or* ***b.*** *NaCl at 150 mM; the intensity losses concern mostly residues in the extended acidic domain, between residues 200 and 300, and are quite attenuated at higher salt concentration.*

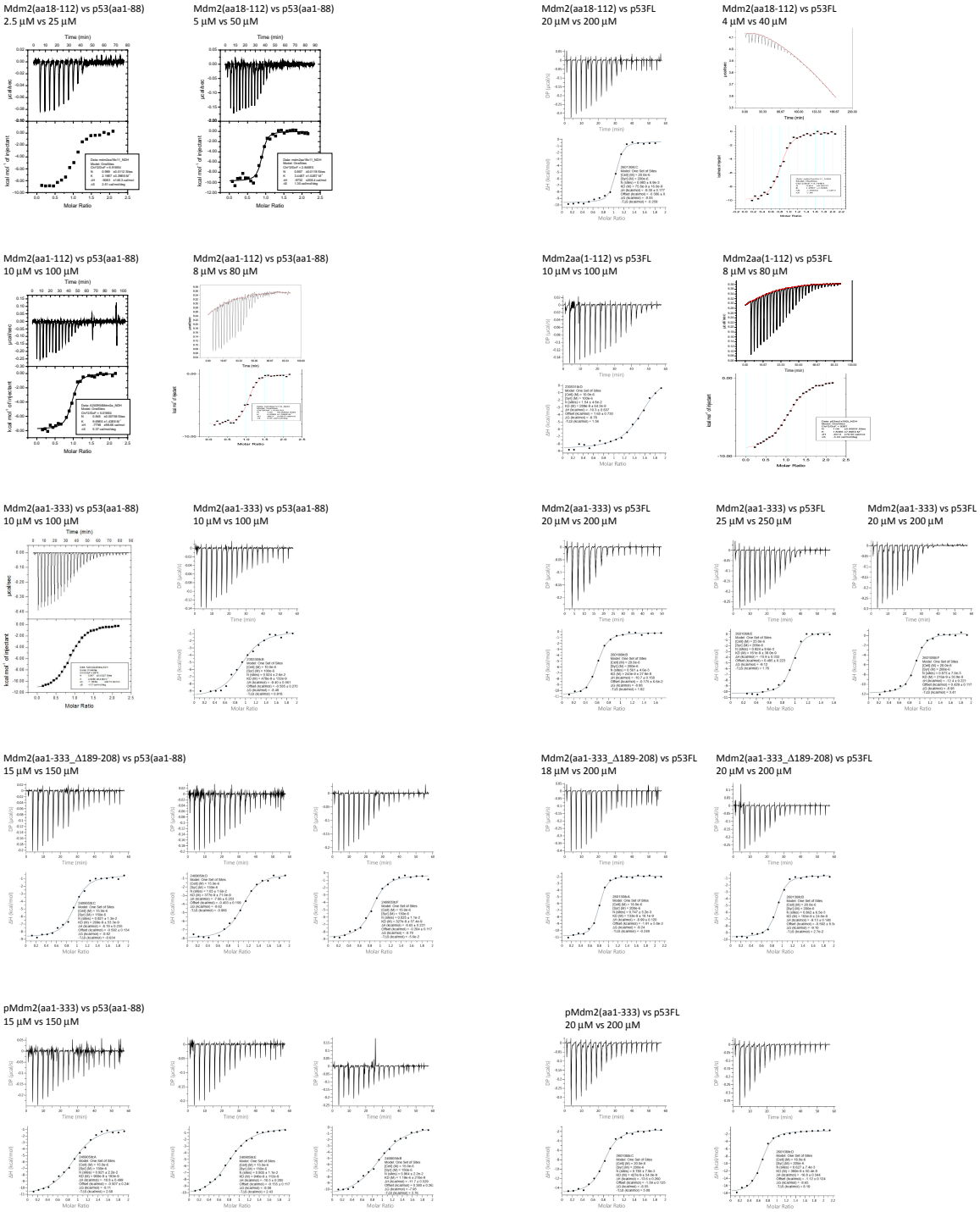

Supplementary Figure 15: *ITC raw data and titration fitting of the various Mdm2 and p53 constructs studied in this study; experiments were carried out using machines of different generations, with different sensitivities, sample volumes and analyzed using softwares also of different generations, which explains some variations in the display between the panels.*

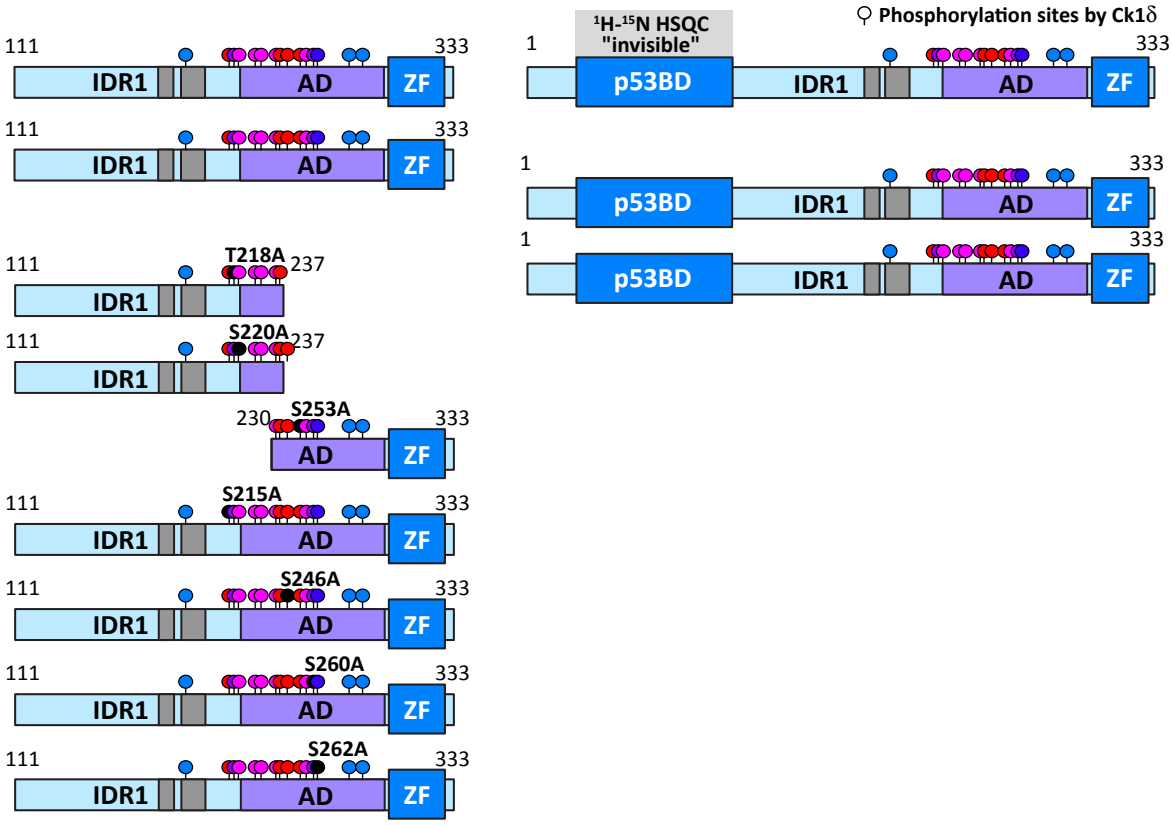

Supplementary Figure 16: *Primary structures of the recombinant Mdm2 constructs produced and analyzed in this study; phosphorylation sites are shown, but we examined both non-phospho- and phospho-forms.*

References

1. Waterhouse, A. M., Procter, J. B., Martin, D. M. A., Clamp, M. & Barton, G. J. Jalview Version 2—a multiple sequence alignment editor and analysis workbench. *Bioinformatics* **25**, 1189–1191 (2009).
2. Kuraku, S., Zmasek, C. M., Nishimura, O. & Katoh, K. aLeaves facilitates on-demand exploration of metazoan gene family trees on MAFFT sequence alignment server with enhanced interactivity. *Nucleic Acids Research* **41**, W22–W28 (2013).
3. Katoh, K., Rozewicki, J. & Yamada, K. D. MAFFT online service: multiple sequence alignment, interactive sequence choice and visualization. *Briefings in Bioinformatics* **20**, 1160–1166 (2019).
4. Madeira, F. *et al.* The EMBL-EBI Job Dispatcher sequence analysis tools framework in 2024. *Nucleic Acids Research* **52**, W521–W525 (2024).
5. Fenton, M. *et al.* The MDMX Acidic Domain Uses Allovalency to Bind Both p53 and MDMX. *J. Mol. Biol.* **434**, 167844 (2022).
6. Song, Q., Liu, X.-Q. & Rainey, J. K. The MDMX acidic domain competes with the p53 transactivation domain for MDM2 N-terminal domain binding. *Biochim. Biophys. Acta - Mol. Cell Res.* **1869**, 119319 (2022).
7. Tamiola, K. & Mulder, F. A. A. Using NMR chemical shifts to calculate the propensity for structural order and disorder in proteins. *Biochem. Soc. Trans.* **40**, 1014–1020 (2012).
8. Nielsen, J. T. & Mulder, F. A. A. CheSPI: chemical shift secondary structure population inference. *J Biomol Nmr* **75**, 273–291 (2021).